Biochimica et Biophysica Acta, 396 (1975) 149—154

BBA Report

BBA 41273

MULTICHANNEL MICROSPECTROFLUOROMETRY FOR TOPOGRAPHIC AND SPECTRAL ANALYSIS OF NAD(P)H FLUORESCENCE IN SINGLE LIVING CELLS

ELLI KOHEN*, JOSEPH G. HIRSCHBERG, CAHIDE KOHEN, ALAIN WOUTERS, ALBERT PEARSON, JEAN-MARIE SALMON and BO THORELL

Papanicolaou Cancer Research Institute and Laboratory of Optical Physics and Astrophysics, University of Miami, Miami, Fla. (U.S.A.)

(Received April 25th, 1975)

Summary

Starting from a previously described prototype microspectrofluorometer a more versatile apparatus has been developed with rapid optional operation on a topographic mode for the simultaneous multisite evaluation of NAD(P) reduction-reoxidation transients or on a spectral mode for the analysis of natural and exogenous fluorochromes, in single living cells. On the topographic mode, a detailed kinetic analysis of NAD or NAD P-linked dehydrogenases can be made from 50—100 cell points simultaneously via automatic recording of topographic scans up to 16 times a second, in correlation with microelectrophoretic intracellular injection of metabolites (e.g. nearly immediate response to glucose 6-phosphate, 20—25 s delay for 6-phosphogluconate). Rapid shifts from topographic to spectral operation make possible the detection of a change in fluorescence intensity at a specific intracellular site and the immediate verification of its nature (NAD(P)H or exogenous fluorochrome) by spectral observation,

Multichannel microspectrofluorometry [1,2] with low-light-level camera tubes has allowed the study of metabolic transients, e.g. NAD(P) reduction-reoxidation, due to intracellular microelectrophoretic addition of metabolites, e.g., glucose-6-*P*. The method exhibited capability in the detection of biochemical interactions throughout the living cell simultaneously, also in correlation with intracellular topography (i.e. topographic mode) or spectral properties of the emission associated with intracellular fluoro-

*Adjunct Faculty, Department of Physiology and Clinical Faculty, Department of Pathology, School of Medicine.

chromes (i.e. spectral mode).

While the original prototype of the microspectrofluorometer [3,4] helped to establish the principle of such determinations at high temporal (e.g. 32 ms) or structural resolutions (e.g. a few μm cell regions), the transition from a spectral to a topographic model of operation (or vice versa) was elaborate with limitations in spectral resolution and topographic imaging on detector elements. This necessitated the development of a more versatile system, (Figs 1A and B) with rapid optional transitions from topographic to spectral mode (or vice versa). The spectral and/or the structural resolution was pushed to the limits of detection in terms of quantum noise, as will be described below.

The fluorescence excitation and the microscopic arrangement, down to the image plane at the camera aperture of the Leitz-Ultropak-Unitron system used for such studies, has been reported earlier [5]. The magnification is 225 × : (75 ×) objective and a 3 × lens for the formation of the secondary image. A rectangular diaphragm adjustable along two perpendicular coordinates from 10 mm to 50 μm is placed in the image plane to function as a slit (Fig. 1A). This slit is perpendicular to the unilinear multichannel array of the low-light level camera tube for operation in the spectral model and parallel to the channel array for the topographic mode (Fig. 1B). Following the slit, a 160 mm lens is placed in the optical path at such distance that the image in the slit corresponds to the focal plane of the lens. A focusing mount provides range for adjustment. A wheel with five turrets rotates past the lens to allow optically centered alignment for five possible options: Amici prisms of different resolutions are mounted in four of the turrets, thus providing a range of spectral options; the fifth turret has no prism and provides the topographic option. The wheel is followed by a Schneider-Varagon zoom lens set to infinity and with a focal length from 16 to 80 mm.

The detector front is placed on the image plane of the zoom. The 500 detector channels arranged on a unilinear array have a width of 25 μm each and a length of 5 mm (half of the length is left in the dark, for automatic subtraction of the dark current signal).

A system of "detentes" permits the setting of the zoom at focal lengths: 16, 20, 25, 35, 50, 65, and 80 mm which correspond to demagnifications of 10, 8, 6.4, 4.6, 3.2, 2.5, and 2, with respect to the fluorescence image at the slit. Thus, on the topographic option the structural resolution of cell elements viewed by individual channel elements may be adjusted by the zoom lens; on the spectral mode the dispersion depends upon the choice of the Amici prisms and the setting of the zoom.

On the topographic mode with 225 × magnification on the microscopic system, a 10 mm slit parallel to the channel array corresponds to a cell region measuring 10000/225 = 44 μm. With the zoom set at 80 mm i.e. a demagnification of 2 from microscopic image plane to zoom image plane, 44 μm in the microscopic field will correspond to 5 mm (or 5000 μm) on detector channels, i.e. 44 μm cell region will fall on 5000/25 = 200 channels. The cell region viewed by each channel will correspond to a strip about 0.2 μm wide (the strip length being determined by the setting of the slit in the coordinate parallel to channel length, i.e. perpendicular to channel array).

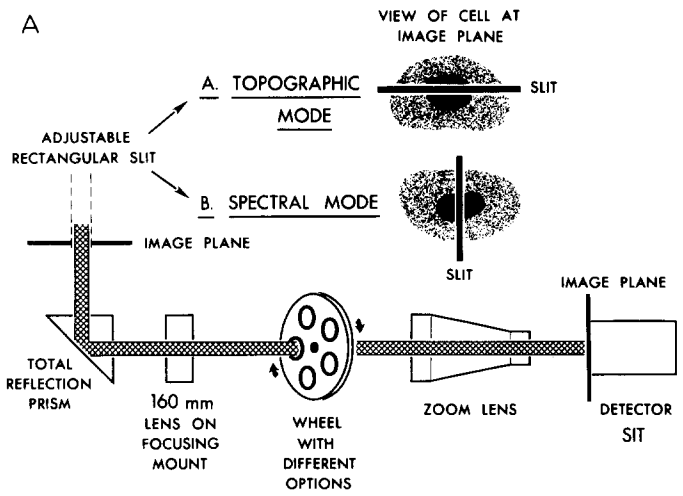

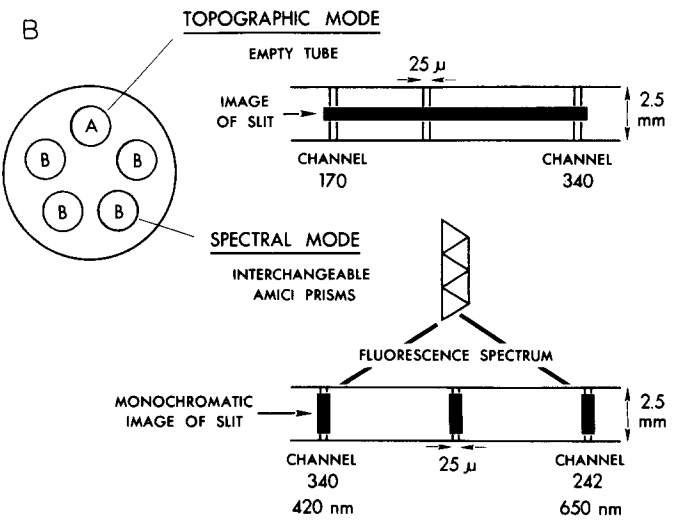

Fig.1. (A) Schematic diagram of the optical arrangement for optional operation on topographic or spectral mode. The adjustable rectangular slit is placed on the image plane of the microscopic arrangement (Leitz-Ultropak mounted on Unitron inverted metallurgical microscope) for the microspectrofluorometer. The view of the cell at the image plane and the slit position are shown for both modes of operation. The 160 nm lens is placed on the optical path at such distance that the image in the slit corresponds to the focal plan of the lens. The wheel with the different options includes five turrets, each one of which may be aligned on the optical path at will. Four of the turrets include Amici prisms of different resolution, thus providing a range of spectral options. The fifth turret has no prisms and provides the topographic option. The topographic or spectral fluorescence image is focused on the unilinear channel array of the detector, SIT = silicon intensified tube. The topographic or spectral dispersion is adjusted by the zoom with focal length from 16 to 8 mm. (B) The imaging of the slit on the unilinear channel array of the detector (silicon intensified camera tube) for operation on topographic (parrallel to channel array) or spectral (perpendicular to channel array) mode. On the left upper corner there is a cross section of the five-option turret arrangement (see Fig. 1A) which allows the positioning on the optical path: either of a Amici prism (B) of selected resolution for spectral operation or of an empty turret (A) for topographic operation.

In the spectral mode, with the Amici prism exhibiting low dispersion the NAD(P)H emission from ≈ 610 nm to 425 nm (maximum at ≈ 470 nm) is dispersed on 37 channels for the zoom set at 16 mm and respectively 46, 58, 810, 116, 150, 185 channels for settings at 20, 25, 35, 50, 65, and 80 mm. A slit setting of ≈ 1.25 provides a spectral resolution comparable to that obtained with the prototype [3,4]. However, the slit may be set to 0.5 mm for cells with higher NAD(P)H fluorescence or having accumulated fluorochromes with higher quantum yield (e.g. polycyclic hydrocarbons) in which case a spectral resolution of about 6 nm is obtained.

With Amici prisms exhibiting larger dispersion, a larger portion of the spectrum in the visible falls outside the 12.5 mm range covered by the 500 detector channels and a wedge of selected dioptry has to be placed on the light path to spread on detector channels a selected portion of the spectrum. Wavelength calibration is made using standard spectral lines: e.g. mercury, helium, or mercury-neon emission. The first applications to a biological system were on EL2 ascites cancer cells studying the NAD(P)H transients which follow microelectrophoretic addition of substrate, e.g. glucose-6-*P* [8] or 6-phosphogluconate [9]. In the topographic mode when the cell is aligned in the microscopic field along the projection of the channel array, the multisite fluorescence image prior to addition of substrate, reproduces the intracellular fluorescence distribution in correlation with structural detail. Upon addition of substrate, a huge increase in fluorescence is noticeable, more prominently in the nuclear region (Fig. 2). The performance of the system has been considerably optimized as compared to the original instrument described before, in terms of number of cell sites simultaneously studied and signal-to-noise ratio (e.g. 10 to 1) for operation at maximum temporal resolution. The possibility to obtain multisite fluorescence images from 50—100 points, up to 16 times a second in correlation with automatic data recording, make possible the simultaneous detailed kinetic analysis of NAD

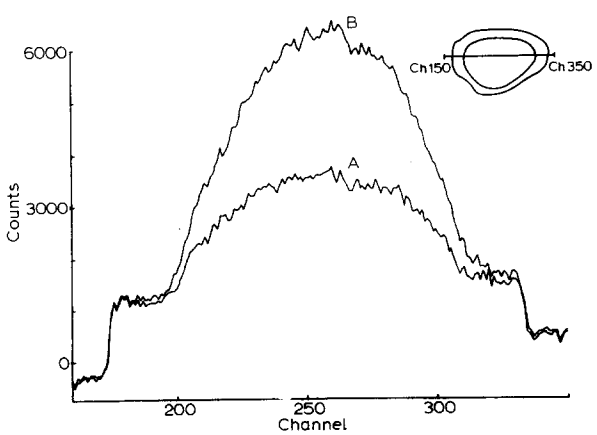

Fig. 2. Topographic fluorescence curves of an EL2 cell, spread on ≈ 160 detector channels: A (before microelectrophoretic intracellular microinjection of glucose-6-*P*), B: ≈ 5 s after glucose-6-P. The nearly vertical rise and descent on both sides of the curve correspond to the slit edges which delimit the microscopic region viewed by the detector channels. 1 count ≈ 1 photoelectron. The huge multichannel (multisite) response to glucose-6-*P* (NAD(P) reduction is seen). Similar changes were obtained in about 50 cells.

or NAD(P)-linked dehydrogenase reactions throughout the cell. Thus, both on the topographic and spectral mode, as compared to the nearly immediate NAD reduction by glyceraldehyde phosphate dehydrogenase [10] observed upon addition of glucose-6-*P* (Fig. 3), a biphasic response (small initially, and larger 15—20 s later) is noticeable with the NAD(P)-linked substrate (6-phosphogluconate) of the hexose monophosphate shunt [11]. The possibility of rapid shifts from a topographic to spectral mode of operation or vice versa, makes feasible the topographic detection of a change in the intensity of fluorescence emission at a specific intracellular site and the immediate verification of its nature (exogenous fluorescent probes [1,12,14]) or NAD(P)H by spectral observation (or vice versa).

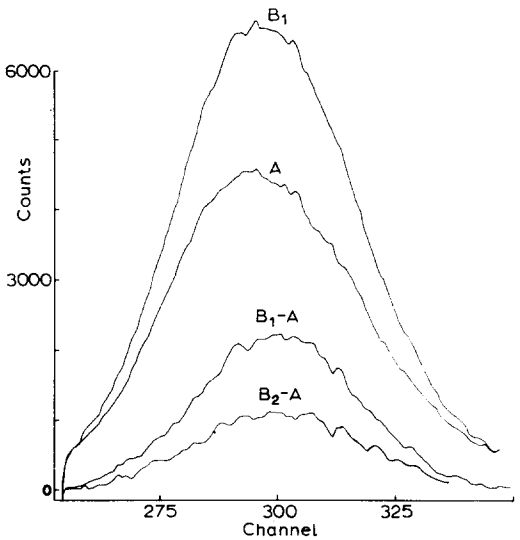

Fig. 3. Fluorescence spectra of an EL2 cell recorded from ≈ 426 nm (channel 340) to ≈ 608 nm (channel 260). A = before intracellular microelectrophoretic injection of glucose 6-phosphate, B_1 = ≈ 5 s after glucose 6-phosphate, B_1—A = difference spectrum (after glucose-6-*P* minus before) at ≈ 5 s, B_2—A = difference spectrum at ≈ 30 s (starting regression of the glucose-6-*P* response, i.e. reoxidation NAD(P)-reduced by substrate). 1 count ≈ 1 photoelectron. The emission maximum in B_1 is at ≈ 470 nm. The cell was grown for 5 days in 10^{-8} M dibenzo(a,e)fluoranthene, a condition which was observed to enhance the catabolism of micorinjected glucose-6-*P*. However, similar spectra were obtained with glucose-6-*P* in several hundred EL2 cells under various conditions.

This work was supported by American Cancer Society Grants BC-15B (Martha S. Blair Memorial Grant for Cancer Research) BC-15C and BC-15D (Thomas E. Raffington Memorial Grant for Cancer Research), and NIH General Research Support Grants to the Papanicolaou Cancer Research Institute GRSG 5 S01 RR05690-04 & 05.

References

1 Kohen, E., Kohen, C., Salmon, J.M., Bengtsson, G. and Thorell, B. (1974) Biochim. Biophys. Acta 362, 575—583
2 Kohen, E., Thorell, B., Salmon, J.M. and Kohen, C. (1973) Rev. Sci. Instr. 44, 1784—1785
3 Kohen, E., Thorell, B., Kohen, C. and Salmon, J.M. (1974) Advances in Biological and Medical Physics, Vol. 15, pp. 271—297, Academic Press, New York

4 Kohen, E., Thorell, B., Kohen, C. and Salmon, J.M. (1974) Techniques of Biochemical and Biophysical Morphology, Vol. 2, pp. 157—195, John Wiley and Sons, Inc., New York
5 Kohen, E., Kohen, C. and Thorell, B. (1972) Biochim. Biophys. Acta 286, 189—196
6 Velick, S.F. (1958) J. Biol. Chem. 233, 1455—1467
7 Winer, A.D., Schwert, G.W. and Millar, D.B.S. (1959) J. Biol. Chem. 234, 1149—1154
8 Meyerhof, O. and Wilson, J.R., (1949) Arch. Biochem. Biophys. 21, 1—34
9 Pontremoli, S., de Flora, A., Grazi, E., Mangiarotti, G., Bonsignore, A. and Horecker, B.L. (1961) J. Biol. Chem. 236, 2975—2980
10 Chance, B. and Hess, B. (1959) J. Biol. Chem. 234, 2421—2427
11 Katz, J., Landau, B.R. and Bartsch, G.F. (1966) J. Biol. Chem. 241, 727—740
12 Salmon, J.M., Kohen, E., Kohen, C. and Bengtsson, G. (1974) Histochemistry 42, 61—74
13 Salmon, J.M., Kohen, E., Kohen, C. and Bengtsson, G. (1974) Histochemistry 42, 75—84
14 Salmon, J.M., Kohen, E., Kohen, C. and Bengtsson, G. (1974) Histochemistry 42, 85—98